

# ALOS PALSAR Investigation of Coastal Geomorphologic Mapping

PI No. 120

*Joong-Sun WON*

Earth System Sciences, Yonsei University  
134 Shinchon-dong Seodaemun-gu, Seoul 120-749, Korea  
E-mail: [jswon@yonsei.ac.kr](mailto:jswon@yonsei.ac.kr)

## ABSTRACT

High precision DEM of a tidal-flat is valuable to coastal management as well as pure scientific interest including erosion and sedimentation rate study. Geomorphologic mapping in coastal zone is, however, complicated by the rapid and significant changes on many fluvial forms and poor topographic expression of the landform. Three space-borne SAR systems including ALOS PALSAR, TerraSAR-X and ERS-ENVISAT tandem mode were examined for effectiveness of interferometry at the west coast of Korean Peninsula. Tide level and tidal conditions such as ebb or flood tide play important role in coherence of radar interferogram. A long antenna baseline and a short temporal baseline are required for coastal applications. ALOS PALSAR with a 43 day repeat cycle produced coherent pairs over vegetated land but was not very effective at tidal flats. The coherence was ranging from 0.3 to 0.5. ALOS PALSAR DEM reflects the surface variation reasonably with a standard deviation of 7.4 m. The eleven day repeat cycle of TerraSAR-X may not be perfect for coastal observation but shorter than ALOS PALSAR. The high resolution capability with salt marsh sensitive X-band observation is also a great advantage for coastal area study. However, X-band was sensitive to moisture content in troposphere. The seasonal variation was very common in TerraSAR-X pairs and winter was better to observe at least in Korea according to vapor content. TerraSAR-X was also useful for salt marsh mapping with a strong backscattering by halophyte. In addition, the high resolution X-band is very good in discrimination of water and exposed tidal flat. The ERS-ENVISAT cross interferometry was most effective with a long baseline and only 30 minute temporal baseline for tidal flat DEM generation. Detailed topographic variation were well rendered by the ERS-ENVISAT cross interferometry. In summary, a cross interferometric system with a synchronized two or more would be an optimal spaceborne SAR system for coastal study.

## 1. INTRODUCTION

A coastal zone is the interface between the oceans and seawater, and is continually changing because of the dynamic interaction between the oceans and the land. Waves and winds along the coast are both eroding rock and depositing sediment on a continuous basis, and rates of erosion and deposition vary considerably from day to day along such zones. Tides, currents, and waves bring energy to the coast, and thus we start with these three factors. Intertidal sediment distribution is an important factor in the understanding of coastal erosion, estuarine ecology, and pollution processes, and it is an indicator of morphological change (Rainey et al., 2000; Beanish et al., 2002). High precision DEM of a tidal-flat is valuable to coastal management as well as pure scientific interest including erosion and sedimentation rate study. Geomorphologic mapping in coastal zone is, however, complicated by the rapid and significant changes on many fluvial forms and poor topographic expression of the landform. The timely updating of coastal landform is of critical not only for geomorphology itself but also for geologic process study, environmental management, and

sustainable development. However, there is practical difficulty in delineating clear-cut boundaries for terrain forms particularly for coastline and associate landforms. Consequently many parts of the world, the coastline and geomorphologic features of inter-tidal zone in pre-existing maps are often not accurate enough.

Vast tidal flats (about 6000 km<sup>2</sup>) are developed particularly along the west and south coast of the Korean Peninsula. The Korean tidal flats have two distinctive features: (1) they are composed of fine-grained sediments, and (2) sand bars are very poorly developed. From remotely sensed data it is generally much more difficult to classify the surface sediment distribution of fine grains than coarse grains (Ryu et al., 2004). Generally, tidal flats show dynamic morphologic changes that arise from high tidal energy and sediment transportation. The driving force of coastal changes results from sediment budget processes, tectonic processes, marine energy processes, relative sea-level movements, and human impacts. Sedimentation and erosion, or their combination on the Korean tidal flats is significant due to the high tidal energy. Land reclamation, which has been conducted on a large scale, has also accelerated environmental changes in

the tidal flats. Sediment budget is very important, especially to ecological systems. The sedimentation budget can be estimated if the total morphologic change that occurred in a certain period is measured, and if the types of sediments are discriminated.

The objectives of the research are to apply ALOS and other available remote sensing data to coastal geomorphologic mapping and sediment type classification in coastal region, which eventually is to provide the information of sedimentation budget in a coastal area. PALSAR interferometry and waterline method are main tools for coastal geomorphologic mapping in this study.

## 2. STUDY AREA AND APPLIED METHOD

### 2.1 Study area

The study area was the Kyunggi Bay located in the west coast of Korean Peninsula as in Figure 1. Three test sites were particularly selected for the study including Ganghwado tidal flats, Siwha, and Hwaong-lakes (Figure 2) within the Kyunggi Bay. Ganghwa tidal flat in Figure 2(A) is an open type and one of the biggest tidal flats on the west coast of Korea and is the first tidal flat as a national preservation area. Substantial amount of sediments are supplied from the Han River (or Han-gang). The sediment distribution in Kanghai tidal flat can be classified into mud flat, mixed flat and sand flat.

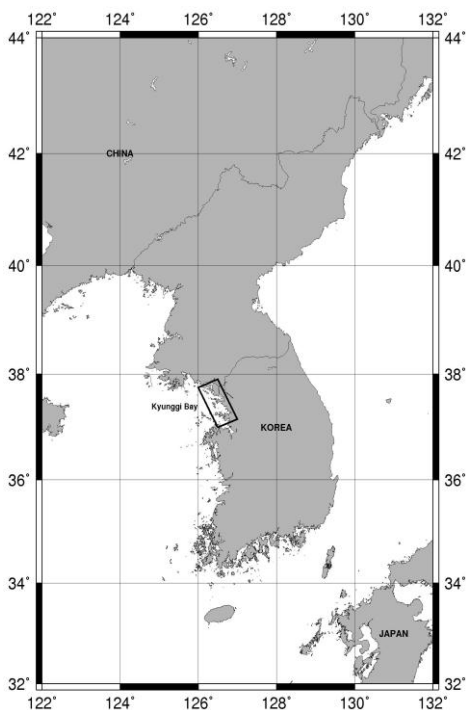


Figure 1. Location map of the study area

Shiwha Lake in Figure 2(B) is close to the cities of Ansan, Siheung and Whasung. This lake is bounded by a dike with a total length of 12.6 km as a part of the 173 km<sup>2</sup> land development plan. Shiwha Lake is mainly composed of mud flat, sand and mixed flat. Hwaong Lake in Figure 2(C) is a large impounding lake, constructed by a land reclamation project for the development of the coastal region of Nanyang Estuary, nearshore the west coast of Korea. The dike construction was completed in March 2002. Hwaong Lake is of mud flat (Hong, 2006).

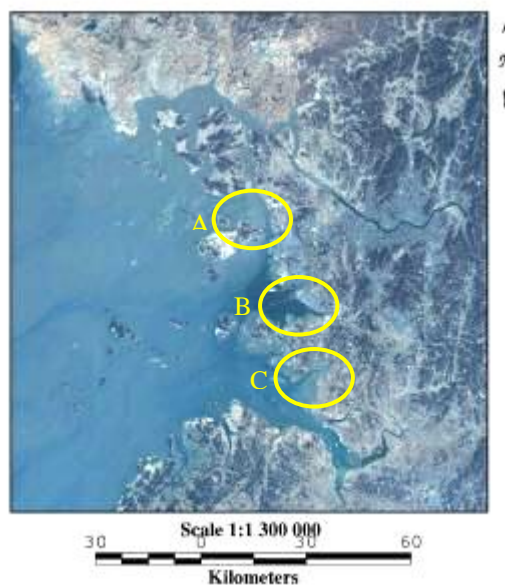


Figure 2. LANDSAT ETM image overlaid with three test sites. The 'A' is the area of the Kanghai tidal flat, 'B' the area of Shiwha Lake and 'C' the area of Hwaong Lake (Choi *et al.*, 2007)

### 2.2 Applied method and data

SAR interferometry using space-borne SAR have recently become one of the most effective tools mapping topography and monitoring surface change due to landslides, earthquakes, subsidence and volcanic eruption. Departures from the regular interference pattern can be used to determine the elevation of the reflecting points relative to some selected datum. ALOS PALSAR advantage over other current satellite SAR systems is its low radar frequencies. L-band observation is much less sensitive to temporal decorrelation than C-band. Temporal decorrelation problem in coastal region is serious because features on land and tidal-flat surface change in a relatively short period. Speckle is also better in L-band observation. A dual-frequency GPS receiver on ALOS would provide baseline information with required precision. Provided that baselines are close enough, mismatching of Doppler centroids in master and slave images can easily be corrected by a filtering process. Thus Doppler centroid matching process in raw signal

processing step is not required in our application. Our own interferometric processor coded in Matlab and C-code designed for DEM estimation and differential interferometry were used, and tested using ERS, RADARSAT, and JERS-1 SAR data. The processor includes most interferometric processing steps such as image co-registration, spectral filtering in both azimuth and range, estimation of the interferometric baseline, correction of the interferogram with respect to the "flat earth" phase contribution, and various phase unwrapping algorithms. Through our previous experiments, we found that: i) a properly designed azimuth filter based upon the antenna characteristic improves coherence considerably; ii) a co-registration process combined by fringe spectrum and amplitude cross-correlation techniques results in optimal matching. The key step of this application would be a co-registration step because there is a lack of distinguishable matching points. However, inter-tidal channel, sandbanks, and artificial features were exploited for image co-registration. As similar to RADARSAT fine mode image, inter-tidal channels in mudflat can easily discriminated in a ALOS PALSAR image and backscattering is relatively high depending on channel and antenna look direction. Sandbanks can also be utilized as GCP points, and there exist some artificial features such as aqua-culturing gear.

If the accuracy of ALOS baseline information is an order of a few meters, the DEM accuracy can be fitted to an order of a few meters in coastal. In this study, we conducted DEM estimation from PALSAR pairs and review the applicability of differential interferometric technique. Coherence map from interferometric pairs was also generated to detect coastline and geomorphologic change. The results were compared with TerraSAR-X and ERS-ENVISAT cross interferometry.

A total of nineteen ALOS PALSAR data sets had been acquired over the study area between 2007 and 2010. Details of the data characteristics are summarized in Table 1. All data were collected by ascending mode, and two data sets were in full polarization mode with a different incidence angle. Baselines and the corresponding ambiguity heights were calculated from the seventeen data sets in FBS and FBD modes. Table 2 lists the ambiguity heights calculated from the seventeen data sets.

### 3. RESULT

Coastal DEM through radar interferometry is difficult to construct mainly because of temporal decorrelation due to different tide levels and fast changes in surface conditions. In this study, three results obtained from ALOS L-band PALSAR, TerraSAR-X, and ERS-ENVISAT tandem pairs were examined and compared with each others.

**Table 1. ALOS PALSAR data used in this study**

| No. | Orbit     | Mode / Incidence angle | Date       | Tide Level (cm) |
|-----|-----------|------------------------|------------|-----------------|
| 1   | Ascending | FBS / 34.4°            | 2007-01-04 | 204             |
| 2   |           |                        | 2008-01-07 | 197             |
| 3   |           |                        | 2008-02-22 | 172             |
| 4   |           |                        | 2008-04-08 | 152             |
| 5   |           |                        | 2009-01-09 | 222             |
| 6   |           |                        | 2009-02-24 | 128             |
| 7   |           |                        | 2010-01-12 | 283             |
| 8   |           |                        | 2011-01-15 | 413             |
| 9   |           | FBD / 34.4°            | 2007-05-22 | 527             |
| 10  |           |                        | 2007-07-07 | 700             |
| 11  |           |                        | 2007-08-22 | 641             |
| 12  |           |                        | 2007-10-07 | 328             |
| 13  |           |                        | 2008-07-09 | 642             |
| 14  |           |                        | 2009-07-12 | 339             |
| 15  |           |                        | 2009-08-27 | 670             |
| 16  |           |                        | 2009-10-12 | 656             |
| 17  |           | PLR / 21.4°            | 2010-05-30 | 187             |
| 18  |           |                        | 2007-04-13 | 417             |
| 19  |           |                        | 2009-04-18 | 529             |

#### 3.1 ALOS PALSAR

L-band interferometry is generally superior in terms of temporal decorrelation to X- or C-bands in land particularly where the surface is covered with vegetation. However, feasibility of L-band interferometry over coastal region and tidal flats has not been well studied. Figure 3 displays examples of ALOS PALSAR interferogram in the study area using the data pairs of August-October 2010 and May-August 2010. The baseline and ambiguity height of the August and October pair (Figure 3(a)) were 194 m and 288 m, respectively. The baseline and ambiguity height of the May and August pair (Figure 3(b)) were 820 m and 73 m, respectively. Due to different ambiguity height, the fringe patterns are different each other. Since topographic variation is relatively low and smooth in coastal region and tidal flats, it is generally recommended to use pairs of a small ambiguity height. Coherence was first examined. Figure 4 shows the coherence map of the 20070522/20070822 pair. The difference of tide level was about 1.14 m. Urban areas generally had high coherence as expected but coherence at hills was relatively low due to seasonal change of vegetation. Coastal region was also of relatively low coherence. Over the tidal flats, variation of coherence was large according to surface conditions.

On the Kanghwa tidal flat, the coherence was relatively low ranging from 0.3 to 0.5. In this area, the surface of tidal flat is largely affected by tidal dynamics and sedimentation/erosion is considerably active during the heavy raining season between June and July. In addition, the tide level was 6.41 m and the exposed bottom surface to the air was not large. The Shiwha Lake and Hwaong Lake are protected by dikes and consequently the surface conditions of tidal flats are largely affected by precipitation rather than tide. The coherences within the two areas were relatively higher ranging between 0.6 and 0.7.

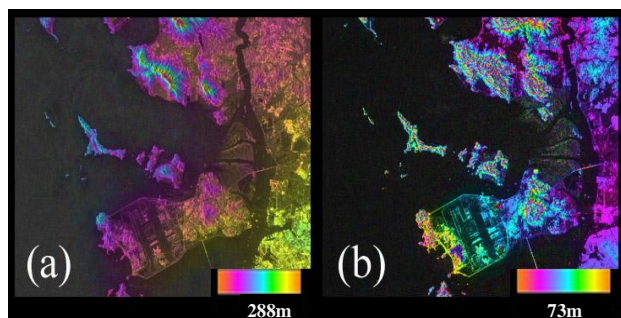


**Figure 3. ALOS PALSAR interterogram in the Ganghwa tidal flat: (a) 070822/071007 pair and (b) 070522/070822 pair**

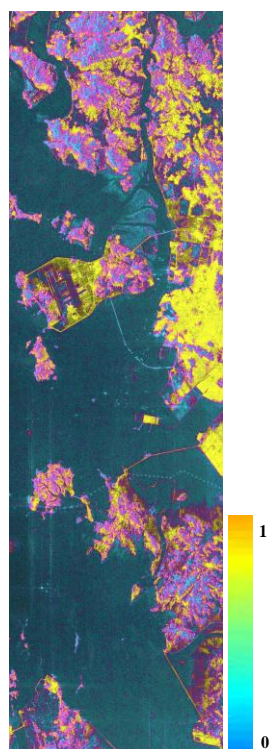


**Figure 4. Coherence map of 2007/05/22 and 2007/08/22 pair (Choi *et al.*, 2007)**

Comparison between the ALOS PALSAR measurements and SRTM DEM was made as shown in Figure 5. Five sub areas were selected at typical topographic features in coastal regions. The five sub areas includes two tidal flats one in Shiwha Lake and the other in Hwaong Lake, one relatively smooth and flat land, one gentle sloped hill, and one relatively steep sloped hill. The sub areas are denoted by red rectangles in Figure 5(A). Since SRTM DEM was constructed by a particularly designed C-band SRTM SAR system with a fixed baseline, the DEM at land should be better than that from ALOS PALSAR in this study. However, SRTM DEM over tidal flats does is not precise

Since the ambiguity height of the ALOS PALSAR in Figure 5(B) was 73 m, topographic details were not well rendered in hills. The largest discrepancy between the two DEMs was observed at the steep hill. In the relatively flat and smooth areas, the correlation between the two results increased. One interesting result was observed in tidal flat. SRTM DEM is relatively smooth in Hwaong Lake tidal flat with a standard deviation of 1.4 m, ALOS PALSAR DEM reflects the surface variation very well with a standard deviation of 7.4 m.

In the coastal regions, topographic height measurement through radar interferometry generally requires 1) a short temporal baseline and 2) a short ambiguity height (or a large baseline). The former is more important because the surface changes are relatively faster than land and considerably affected by tidal conditions. The revisit time of ALOS PALSAR was longer than one month which may not be short enough to construct a coherent interferometric pair. The ambiguity height should be less than 50 m to practically apply to the coastal region, which requires ALOS PALSAR baseline of larger than 1200 m. However, the longer baseline trades off the coherence in coastal region. Thus ALOS PALSAR was not very effective to construct interferometric pairs in coastal regions and particularly in tidal flats. Waterline method should be an alternative approach for tidal flat DEM construction.

**Table 2. Ambiguity height of ALOS PALSAR pairs used in this study**

|          | 20070104 | 20070522 | 20070707 | 20070822 | 20071007 | 20080107 | 20080222 | 20080408  | 20080709 | 20090109 | 20090224 | 20090712 | 20090827 | 20091012 | 20100112 | 20100530 |
|----------|----------|----------|----------|----------|----------|----------|----------|-----------|----------|----------|----------|----------|----------|----------|----------|----------|
| 20070104 |          |          |          |          |          |          |          |           |          |          |          |          |          |          |          |          |
| 20070522 | 29.34    |          |          |          |          |          |          |           |          |          |          |          |          |          |          |          |
| 20070707 | 20.95    | 73.42    |          |          |          |          |          |           |          |          |          |          |          |          |          |          |
| 20070822 | 20.61    | 69.42    | 1301.13  |          |          |          |          |           |          |          |          |          |          |          |          |          |
| 20071007 | 19.24    | 55.95    | 236.07   | 288.39   |          |          |          |           |          |          |          |          |          |          |          |          |
| 20080107 | 16.40    | 37.20    | 75.50    | 80.27    | 111.23   |          |          |           |          |          |          |          |          |          |          |          |
| 20080222 | 13.65    | 25.54    | 39.18    | 40.43    | 47.02    | 81.56    |          |           |          |          |          |          |          |          |          |          |
| 20080408 | 11.99    | 20.29    | 28.06    | 28.69    | 31.86    | 44.69    | 98.85    |           |          |          |          |          |          |          |          |          |
| 20080709 | 37.15    | -139.52  | -48.11   | -46.35   | -39.93   | -29.38   | -21.59   | -17.73    |          |          |          |          |          |          |          |          |
| 20090109 | 104.97   | -40.75   | -26.21   | -25.68   | -23.58   | -19.45   | -15.70   | -13.56    | -57.56   |          |          |          |          |          |          |          |
| 20090224 | 73.23    | -50.31   | -29.84   | -29.16   | -26.48   | -21.39   | -16.94   | -14.47    | -78.69   | 215.19   |          |          |          |          |          |          |
| 20090712 | 33.24    | -237.07  | -56.29   | -53.80   | -44.97   | -31.77   | -22.74   | -18.45    | 302.42   | 46.94    | 61.08    |          |          |          |          |          |
| 20090827 | 27.07    | 380.60   | -91.72   | -85.29   | -64.98   | -40.63   | -26.95   | -21.13    | -98.33   | 35.50    | 43.04    | 146.08   |          |          |          |          |
| 20091012 | 25.68    | 216.02   | -112.35  | -102.85  | -74.70   | -44.23   | -28.49   | -22.05    | 82.16    | 33.14    | 39.62    | 113.03   | 499.54   |          |          |          |
| 20100112 | 22.09    | 91.27    | -388.53  | -292.92  | -141.64  | -61.35   | -34.73   | -25.63    | 54.06    | 27.41    | 31.68    | 65.90    | 120.32   | 158.49   |          |          |
| 20100530 | 16.36    | 37.35    | 75.61    | 80.62    | 114.41   | -2072.17 | 77.17    | -43.10    | 29.14    | 19.11    | 21.10    | 32.25    | 41.41    | 45.19    | 63.22    |          |
| 20110115 | 11.87    | 20.03    | 27.49    | 28.13    | 31.36    | 44.16    | 98.50    | -11189.72 | 17.40    | 13.25    | 14.18    | 18.47    | 21.15    | 22.09    | 25.66    | 43.24    |

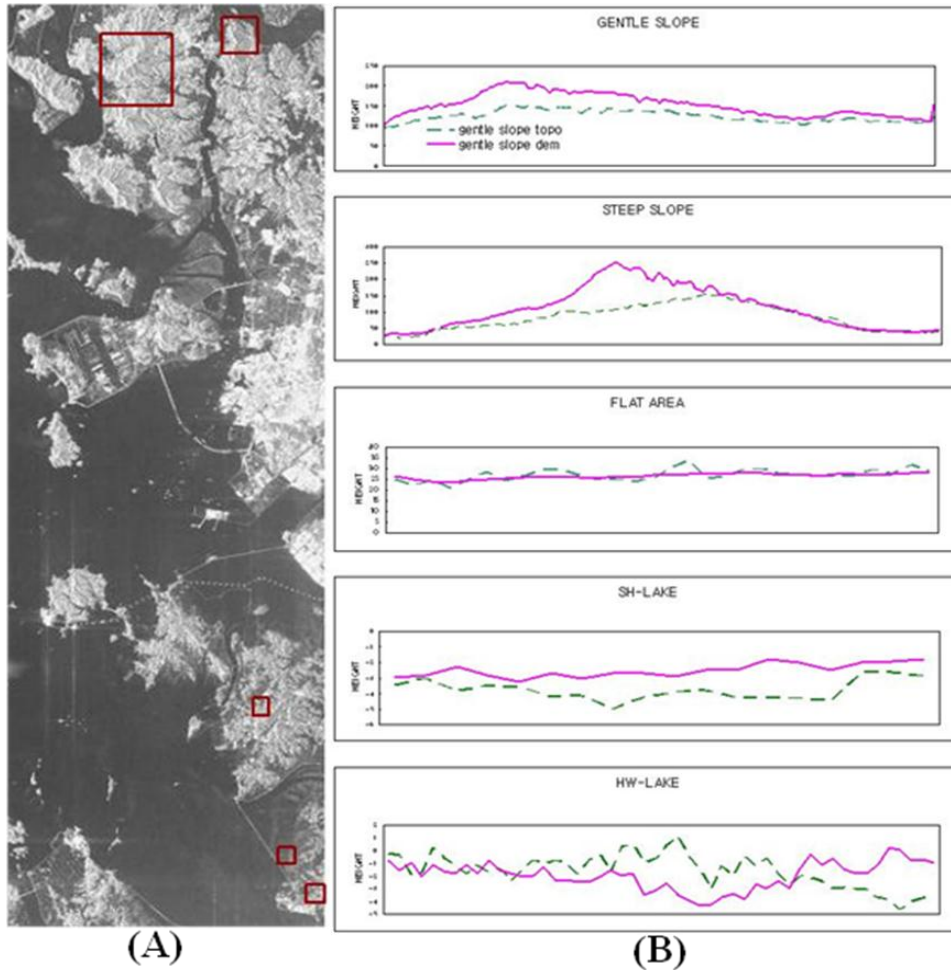


Figure 5. Comparison of topographic height between ALOS PALSAR measurements and SRTM DEM. (A) Location map of DEM comparison. Red box indicates the sub-area where the comparison made. (B) Pink line presents the terrain height from SRTM DEM and green line does terrain height from the ALOS PALSAR 2007/05/22 and 2007/08/22 pair (Choi *et al.*, 2007).

### 3.2 TerraSAR-X interferometry

For comparison with ALOS PALSAR interferometric capability over coastal region, a similar interferometric technique was applied to TerraSAR-X data at the same area. Due to a short wavelength of X-band SAR system, it is well-known that TerraSAR-X data is more subject to temporal decorrelation particularly on the vegetated surface. In addition, the tropospheric vapour effect is also severe to the higher frequencies. On the contrary, TerraSAR-X has advantage of a short of eleven day revisit orbit and high resolution. Coastal region and tidal flats are generally characterized by low vegetation density and higher moisture content in the troposphere in comparison with inland areas. Figure 6 shows typical TerraSAR-X coherence maps in the study area. With the eleven day pairs, TerraSAR-X usually produced higher coherence in winter than in summer due to lower tropospheric vapour (Park *et al.*, 2009). Since there are many controlling factors affecting coherence, it is difficult to conclude tropospheric moisture content alone governs the coherence. However, the seasonal variation is very common in TerraSAR-X pairs and winter is better to observe coastal regions at least in Korea. To our surprise, even fifty-five day pair exemplified in Figure 6(c) is frequently successful to construct coherent interferometric pairs particularly over the areas of salt marsh where halophyte develops. Halophyte species alteration and its demarcation is one of environmental indicators in salt marsh. Therefore, accurate mapping of salt marsh is useful for understanding wetland functions and monitoring their response to natural and anthropogenic actions (Barker *et al.*, 2006).

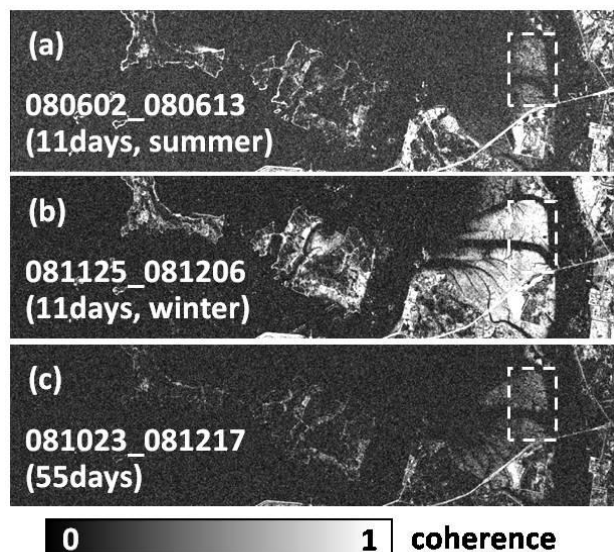


Figure 6. TerraSAR-X coherence map in summer (a) and in winter (b). TerraSAR-X produced generally higher coherence in winter due to lower moisture content in the troposphere. (c) TerraSAR-X coherence map of fifty five day pair. The area of halophyte (boxed area) maintains high coherence even with a long time interval (Park *et al.*, 2009).

Most halophyte species in this area are of *Suaeda japonica* (*S. japonica* hereafter) and *Phragmites australis* (*P. australis* hereafter). *S. japonica* is an annual plant belonging to the family of Chenopodiaceae, and its stem grows up to 50 cm in height. Rapid growth of underground part of *S. japonica* at the beginning stage of the growth could adapt itself to the ebb- and flow environment. After root is fixed firm in the ground (normally during May), the growth of above-ground becomes fast (Lee and Ihm, 2004). The color of short succulent leaves of *S. japonica* changes from green to red with an accumulation of red pigment (betacyanin) (Hayakawa and Agrie, 20010). *P. australis* is also called a common reed and is a perennial grass with annual shoots emerging from perennial underground of rhizomes. It grows up to 3-4 m in height. There are three scattering mechanisms in flooded vegetation: scattering from the canopy, specular scattering from the water, and double scattering between the water and the emergent vegetation (Harritt *et al.*, 2003). It is very interesting to map the areas of salt marsh and their variation by high resolution SAR because their habitat is closely related with sea level change.

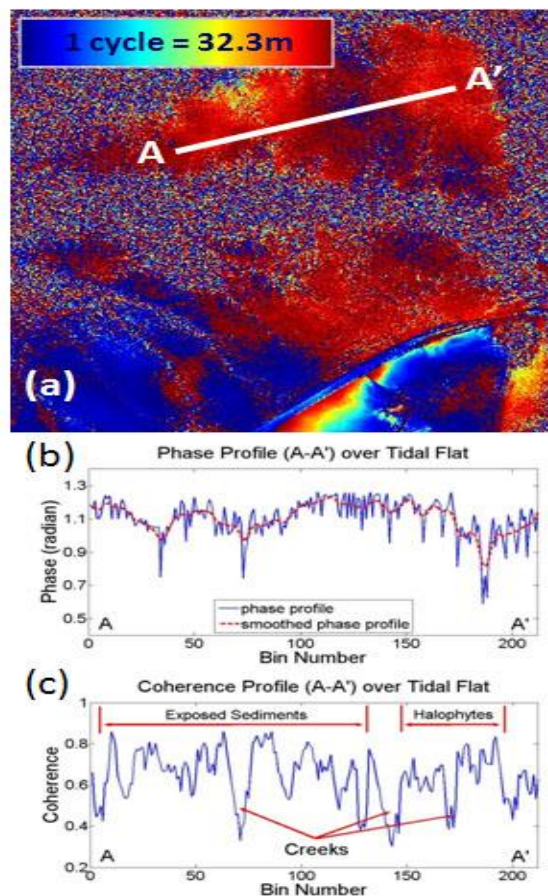


Figure 7. TerraSAR-X interferometry over the tidal flat and salt marsh: (a) Unwrapped interferogram, (b) phase profile along A-A' and (c) coherence profile. The topographic variation in tidal flat is assumed as a smooth surface (Park *et al.*, 2009).



**Figure 8. TerraSAR-X images acquired on 17 April 2009 (left), 28 April 2009 (center), and 14 November 2008 (right). Tide levels were 466 cm, 756cm, and 806 cm, respectively.**

Figure 7 is an example of TerraSAR-X interferometric results using a pair of 12 and 23 October 2008. Due to decorrelation, phase noise was significant compared with land surface. Baseline was 197 m and its ambiguity height was 32.3 m. Tidal levels were 438 cm and 279 cm, respectively, which resulted in relatively large bottom surface exposure. Since the tidal flat topography is reasonable smooth, the radar measured surface can be smoothed by interpolation as in Figure 7(b). The maximum height variation was only 2.6 m with a typical tidal flat topography (Park *et al.*, 2009). Mean coherence was about 0.7 except high land, and areas of halophyte had slightly lower coherence of about 0.6 as shown in Figure 7(c). Tidal channels and creeks should be considered in interpretation because the areas are always filled with water and their walls are steeper than other areas. Although the eleven day repeat cycle of TerraSAR-X is not perfect for coastal observation, its high resolution capability with salt marsh sensitive X-band observation is a great advantage among the current space-borne SAR systems for coastal area study. A synchronized tandem SAR system such as TanDEM-X would be very effective to generate tidal flat DEM if data are acquired under favorable tidal conditions. In addition, the high resolution X-band is very good in discrimination of water and exposed tidal flat as in Figure 8 so that waterline method also works very well. Waterline method is beyond the scope of this report. However, waterline method is very useful in tidal flat DEM construction and the acquisition of a series of data within a short period is a key to the success of the method. Optic images have been dominantly used for the waterline method but a heavy dependency of weather conditions was a main obstacle for acquiring enough number of data sets within a short period. High resolution X-band SAR with a short repeat cycle would provide complementary data sets for the waterline method.

### 3.3 ERS-ENVISAT cross interferometry

We also examined the cross interferometry using ERS-ENVISAT 30 minute tandem pair. Figure 9 shows the

ERS-ENVISAT cross interferogram from a pair of 6 February 2009. ENVISAT was acquired at 10:46 a.m. followed by ERS-2 at 11:16. Due to the minimized temporal decorrelation and a large baseline, an excellent interferogram was obtained over coastal areas and tidal flats. Since the cross interferometry inherently requires a large baseline because of a slight difference of center frequencies between the two SAR systems, it is very useful particularly at flat surface (Colesanti *et al.*, 2003). As seen in Figure 9, fringe patterns are extremely well generated over coastal regions although they are collapsed on high relief. The tidal level was 480 cm at the moment of ENVISAT data acquisition. Coherence and the interferogram quality was the best among the tested three SAR systems; ALOS PALSAR forty-three day, TerraSAR-X eleven day, and ERS-ENVISAT 30 minute tandem pairs.

In addition to tide level, tidal conditions are very important for the quality of interferogram. The data was acquired under flood tide, which is the most favorable condition because of a long exposure time of bottom surface. On ebb tide, there exists a large amount of remnant surface water which reduces coherence as well as backscattering intensity. On the contrary, the remnant surface water significant disappears four to five hours after the first exposure to the air. The area of exposed tidal flat can be inferred by TerraSAR-X in Figure 8. Since the ENVISAT was at the tide level of 480 cm, the status of bottom exposure should be close to the Figure 8(a) which was at 466 cm tide level. The tide level at thirty minutes later on ERS-2 data acquisition was higher about 530 cm which was still close to the Figure 8(a) rather the (b) or (c). However, less tidal flats were exposed to the air than ENVISAT SAR data. It is well worth noting that interferometric fringes at the east side (or landward) were more well preserved than at the west side (or seaward) within the tidal flat in Figure 10. It implies even 30 minutes still reduces coherence according to the tide level change. Figure 10 displays a unwrapped phase profile along a straight line A-A' of a typical tidal flat. The maximum height variation was 2.8 m in Figure 10 and details of topographic variation were well rendered.



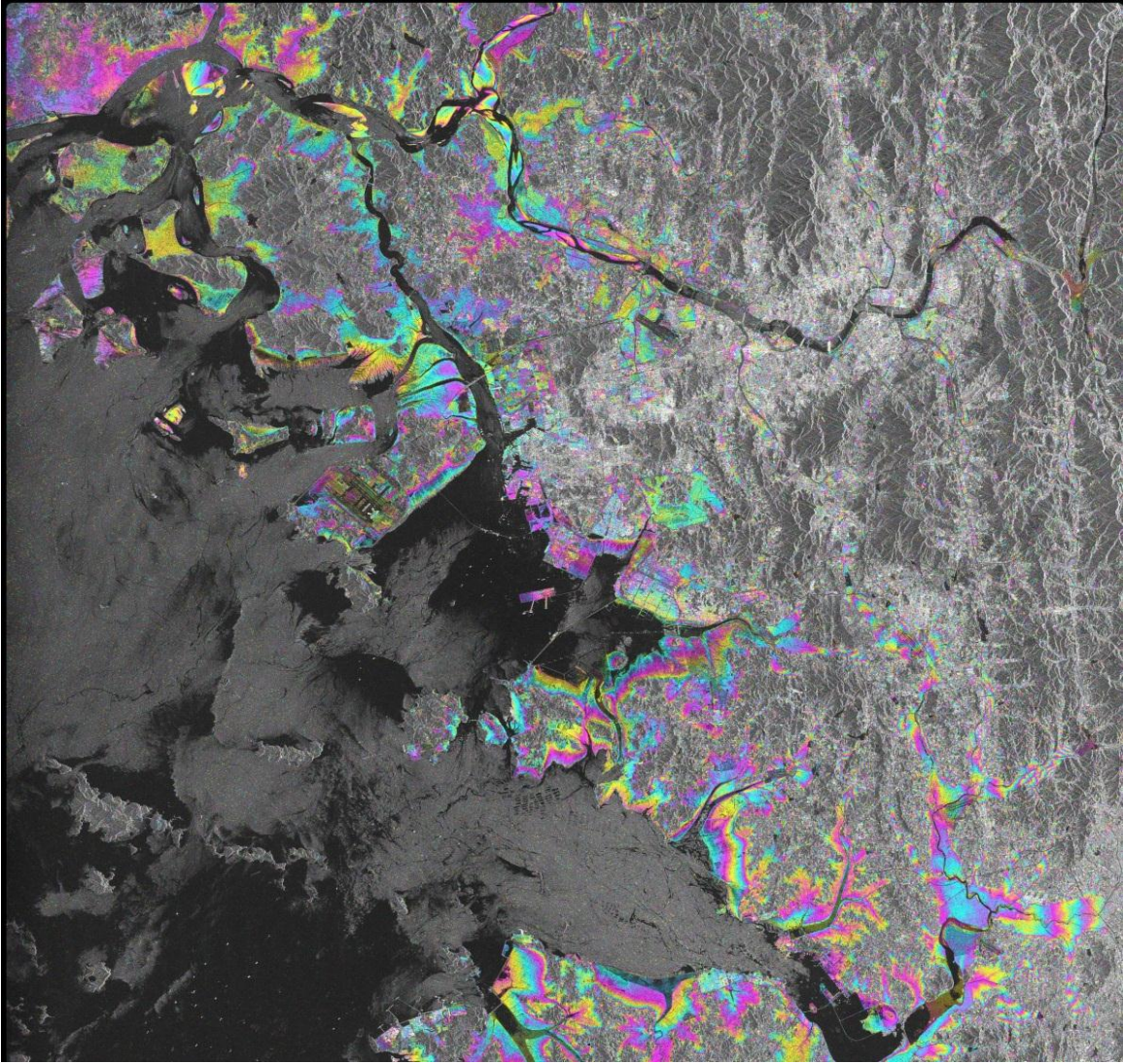


**Figure 9. ERS-ENVISAT cross interferogram from a pair acquired on 6 February 2009.**

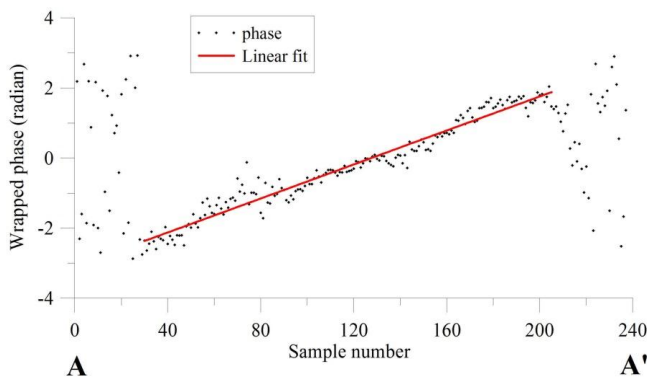
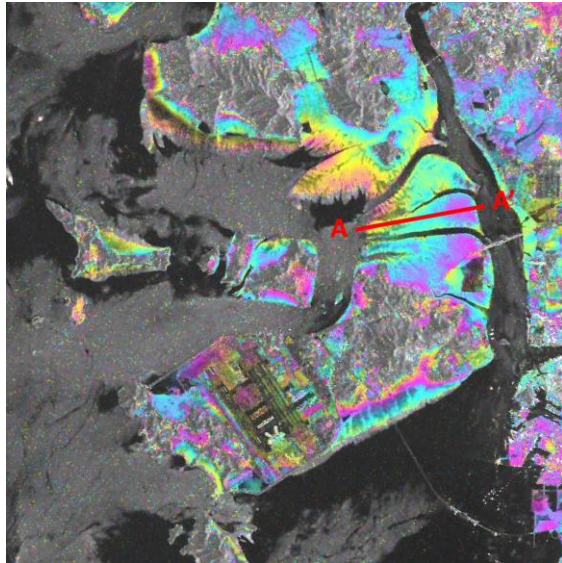


**Figure 10. Interferogram at Ganghwa area (upper) and phase profile along a tidal flat (bottom).**

In short, space-borne radar interferometry over coastal regions and tidal flats requires two system parameters: One is a long antenna baseline and the other is a short temporal baseline. Among the three examined systems including ALOS PALSAR with 43 day pairs, TerraSAR-X 11 day pairs and ERS-ENVISAT 30 minute tandem pairs, the ERS-ENVISAT cross interferometry resulted in the most effective systems satisfying the requirements for coastal and tidal flat DEM generation.

#### 4. CONCLUSION

Coastal and tidal flat DEM is very important to keep monitoring the short and long term changes in coastal regions. Tidal flat DEM is particularly difficult to obtain and the precision of the constructed DEM is often too low to use. Airborne lidar system is available but is not easy to access by public. Three space-borne SAR systems including ALOS PALSAR, TerraSAR-X and ERS-ENVISAT tandem mode were examined for effectiveness of interferometry in coastal regions and tidal flats. Tide level and tidal conditions such as ebb or flood tide play important role in coherence of radar interferogram. For coastal applications, requirements of space-borne radar include two system parameters: One is a long antenna baseline and the other is a short temporal baseline. ALOS

PALSAR with a 43 day repeat cycle produced coherent pairs over landside vegetated areas but was not very effective at tidal flats. While L-band is well known to be robust with a least temporal correlation particularly in the areas covered with trees, the forty-three day repeat cycle was not short enough to maintain highly coherent interferometric pairs in tidal flats. The coherence was relatively low ranging from 0.3 to 0.5. ALOS PALSAR DEM reflects the surface variation reasonably with a standard deviation of 7.4 m.

The eleven day repeat cycle of TerraSAR-X is not perfect for coastal observation but shorter than ALOS PALSAR. The high resolution capability with salt marsh sensitive X-band observation is also a great advantage for coastal area study. However, X-band is more largely affected by moisture content in troposphere than L- or c-band. The seasonal variation is very common in TerraSAR-X pairs and winter is better to observe coastal regions at least in Korea probably due to tropospheric vapor. TerraSAR-X was especially useful for salt marsh mapping because of strong backscattering by halophyte. In addition, the high resolution X-band is very good in discrimination of water and exposed tidal flat.

The ERS-ENVISAT cross interferometry resulted in the most effective systems satisfying the requirements for coastal and tidal flat DEM generation. Since the cross interferometry inherently requires a large baseline to offset the difference of center frequencies between the two SAR systems, it is very useful particularly at flat surface. The only 30 minute time difference was good enough to maintain a coherent interferometric pair in tidal flats as well as coastal regions. Details of topographic variation were well rendered by the ERS-ENVISAT cross interferometry.

In the very near future, a synchronized tandem SAR system such as TanDEM-X would be very effective to generate tidal flat DEM if data are acquired under favorable tidal conditions. In short, a cross interferometric system with a synchronized observation would be the optimal spaceborne SAR system for coastal study.

## REFERENCES

- Hong, S. H., 2006, *Construction of Coastal Digital Elevation Model by InSAR*, PhD Thesis, Yonsei University.
- Massonnet, D., Rabaute, T., Radar Interferometry: Limits and Potential, *IEEE Transactions on Geoscience and Remote Sensing*, 31(2), 455-464, 1993.
- Park, J.-W., Y.-K. Lee, J.-W. Won., “Investigation of Intertidal Zone using TerraSAR-X”, 2009, *Korean Journal of Remote Sensing*, 25(4), 383-389, 2009
- Rainey, M.P., Tyler, A.N., Bryant, R.G., Gilvear, D.J., McDonald, P., The influence of surface and interstitial moisture on the spectral characteristics of intertidal sediment: implications for airborne image acquisition and processing, *International Journal of Remote Sensing*, 21, 3025–3038, 2000.
- Ryu, J.-H., Y.-H. Na, J.-S. Won, R. Doerffer, A critical grain size for Landsat ETMC investigations into intertidal sediments: a case study of the Gomso tidal flats, Korea, *Estuarine, Coastal and Shelf Science*, 60, 491-502, 2004.

### Papers published in the research

- [1] J.-H. Choi, *et al*, “DEM Generation over Coastal Area using ALOS PALSAR Data,” *Korean Journal of remote sensing*, vol.23, no.6, pp.559-566, 2007.
- [2] J.H. Choi, *et al*, “Evaluation of ALOS PALSAR interferometry in the West Coast of Korea: Preliminary Results.” *Proceedings of ISRS 2007*, Jeju, Korea, 2007.